Volume 52 | Number 28 | 11 April 2016 | Pages 4945–5068

ChemComm

Chemical Communications

www.rsc.org/chemcomm

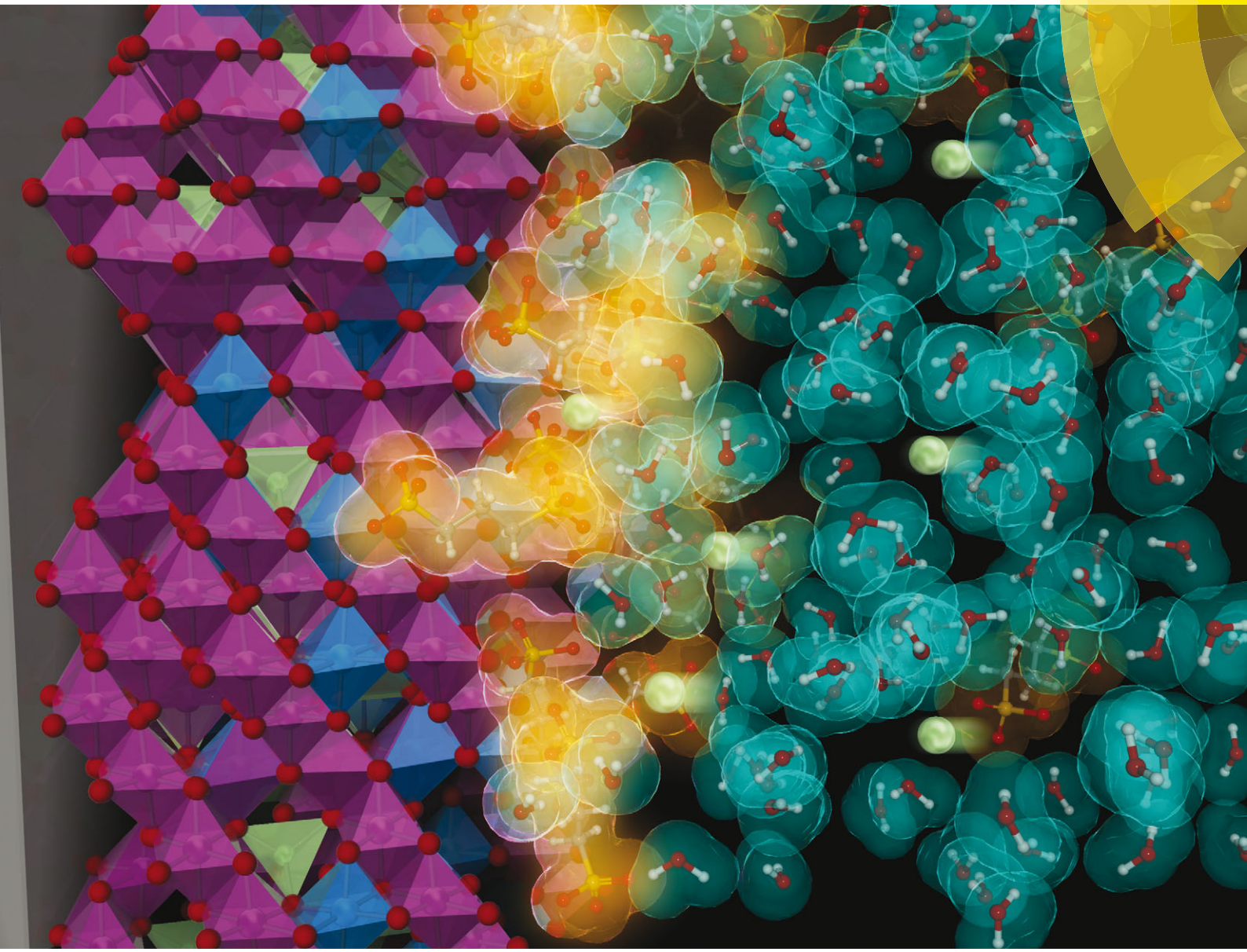

ISSN 1359-7345

ROYAL SOCIETY OF CHEMISTRY

COMMUNICATION

Kohei Miyazaki *et al.*

Enhanced resistance to oxidative decomposition of aqueous electrolytes for aqueous lithium-ion batteries

175 YEARS

ChemComm

COMMUNICATION

View Article Online
View Journal | View Issue

Cite this: *Chem. Commun.*, 2016, 52, 4979

Received 28th January 2016,
Accepted 17th February 2016

DOI: 10.1039/c6cc00873a

www.rsc.org/chemcomm

Enhanced resistance to oxidative decomposition of aqueous electrolytes for aqueous lithium-ion batteries†

Kohei Miyazaki,*[ab] Toshiki Shimada,[a] Satomi Ito,[a] Yuko Yokoyama,[a] Tomokazu Fukutsuka[a] and Takeshi Abe[ab]

An efficient electrolyte solution containing organic sulfonates for use in aqueous rechargeable lithium-ion batteries (ARLBs) is shown to provide a wide potential window and enable a high operating voltage for ARLBs.

Accompanied by the rapid increase in the use of sustainable energy, lithium-ion batteries are finding widespread applications in large-scale energy facilities.[1] Since sustainable energy sources such as solar and wind power suffer from problems related to supply fluctuation, such fluctuation needs to be controlled through the use of buffers, which store and release surplus electric energy.[2] Despite continuous improvements in the safety of lithium-ion batteries, the flammable organic solvents used in the electrolyte have fatal drawbacks, and therefore alternative electrolytes have been studied for large-scale energy-storage applications.[3] In addition to this safety issue, the cost of preparing and handling ultra-dry organic solvents is also a serious concern.

Among alternative electrolytes, aqueous electrolytes could meet the safety and cost requirements of an electrolyte for large-scale battery facilities,[4,5] but their narrow window of electrochemical stability (1.23 V) raises another problem. In 1994, Li *et al.* first reported the concept of aqueous rechargeable lithium-ion batteries (ARLB) using $LiMn_2O_4$ and VO_2(B) as active materials.[6] They demonstrated the continuous charge–discharge performance, but the terminal voltage was limited (less than 1.5 V). Clearly, a narrow electrochemical window would diminish the advantages of plentiful active materials for use in lithium-ion batteries. Considerable effort has been devoted to overcoming the limitation of an electrochemical window, and a few approaches have been found to stabilize aqueous electrolytes. The most common practice is coating of the electrode surface. This is analogous to the formation of a protective layer known as a solid electrolyte interphase (SEI), which mainly forms on graphite electrodes in lithium-ion batteries. Thermodynamically, organic solvents decompose at quite low potentials close to 0 V (*vs.* Li^+/Li), but this process apparently stops after SEI films have sufficiently developed on the electrode surface.[7] Similarly, protective materials can be added to aqueous electrolytes to block the access of water molecules. For example, Stojkovic *et al.* reported that the addition of vinylene carbonate (VC) effectively improved the cycle performance of $Li_{1.05}Cr_{0.10}Mn_{1.85}O_4$ in an aqueous electrolyte.[8]

Another method for obtaining stable aqueous electrolytes is to increase the concentration of salts in the aqueous solutions. In both organic and aqueous electrolytes, it has been found that highly concentrated solutions have some extraordinary physicochemical properties. Jeong *et al.* discovered that organic solutions of propylene carbonate (PC) with a high concentration (2.72 mol dm^{-3}) of lithium bis(perfluoroethylsulfonyl)imide ($LiN(SO_2C_2F_5)_2$, LiBETI) had high tolerance to reductive decomposition at low potentials.[9] Yamada *et al.* also reported that an acetonitrile electrolyte with a high concentration of lithium bis(trifluoromethanesulfonyl)imide ($LiN(SO_2CF_3)_2$, LiTFSI) was highly stable against reduction.[10] Moreover, Suo *et al.* reported a highly concentrated aqueous solution of LiTFSI with a wide window of electrochemical stability.[11] While the mechanism by which solvents are effectively stabilized by a high concentration of salts is not yet clear, these approaches have inspired further explorations of aqueous electrolytes with more stable electrochemical windows. In this communication, we report that the addition of an organosulfate to aqueous electrolytes enhances their resistance to oxidative decomposition. In particular, we investigated the influence of disodium propane-1,3-disulfonate (PDSS) on the properties of aqueous electrolytes. To the best of our knowledge, this is the first report on the use of a high-potential positive electrode material (> 4.5 V *vs.* Li^+/Li) in an aqueous electrolyte (ESI,† Scheme S1).

Spinel-type $LiNi_{0.5}Mn_{1.5}O_4$ thin films were prepared by the sol–gel method. Lithium acetate, nickel(II) acetate tetrahydrate, and manganese(II) acetate tetrahydrate were dissolved in a solution of acetic acid. A methanol solution containing polyvinylpyrrolidone

[a] *Graduate School of Engineering, Kyoto University, Nishikyo-ku, Kyoto 615-8510, Japan. E-mail: myzkohei@elech.kuic.kyoto-u.ac.jp; Fax: +81 75 383 7049*
[b] *Elemental Strategy Initiative for Catalysts & Batteries (ESICB), Kyoto University, Nishikyo-ku, Kyoto 615-8246, Japan*

† Electronic supplementary information (ESI) available: Electrochemical potential window, cyclic voltammograms, XPS results, NMR results. See DOI: 10.1039/c6cc00873a

(PVP, M_w = 55 000) was then added to form a sol of the acetic acid solution. We prepared a precursor sol, in which the molar ratio of CH_3COOLi, $Ni(CH_3COO)_2{\cdot}4H_2O$, $Mn(CH_3COO)_2{\cdot}4H_2O$, CH_3COOH, H_2O, CH_3OH, and PVP was 12 : 5 : 15 : 400 : 200 : 400 : 20. An aliquot of the precursor sol was dropped on a polished Pt substrate, and this was followed by spin-coating at 3000 rpm for 20 s. The Pt substrate with the sol solution was heated in a furnace at 723 K for 1 h, where the temperature was changed at rates of 5 and 1.5 K min^{-1} for heating and cooling. We also examined the use of a gold substrate for the sol–gel method instead of a Pt substrate. Thin-film X-ray diffraction (XRD) measurements were carried out to characterize the obtained sol–gel films, using a CuKα X-ray source.

Electrochemical measurements were performed in both organic and aqueous electrolytes. For the organic electrolyte, we constructed a three-electrode cell with Li metal as both the counter and reference electrodes, and carried out cyclic voltammetry in a PC solution of 1 mol dm^{-3} (M) $LiClO_4$. Electrochemical measurements using the organic electrolyte were conducted in a dry Ar-filled glove box. In aqueous electrolytes, Ag/AgCl and Pt mesh were used for the reference and counter electrodes. We examined five aqueous solutions for use as electrolytes: 0.5 M $LiNO_3$, saturated $LiNO_3$, 0.5 M $LiNO_3$ with saturated PDSS, 0.25 M Li–PO_4 buffer consisting of LiOH and H_3PO_4 with a molar ratio of 3 : 2 (pH 7), and 0.25 M Li–PO_4 buffer with saturated PDSS.

In addition, we investigated the electrochemical potential windows of the electrolytes using a rotating-disk electrode (RDE) of platinum with a rotation speed of 400 rpm. Linear sweep voltammetry was carried out in electrolyte solutions of 0.5 M $LiNO_3$ and 0.25 M Li–PO_4 buffer with saturated PDSS.

To characterize the electrode surface, X-ray photoelectron spectroscopy (XPS, ULVAC-PHI Model 5500) was carried out before and after the electrochemical measurements. Spin–spin relaxation time (T_2) was measured using the ^{1}H NMR Carr–Purcell–Meiboom–Gill (CPMG) method (XiGo Nanotools, Acorn Drop) to characterize the bulk properties of PDSS solutions. The viscosity of PDSS aqueous solutions was measured with an automated microviscometer (Anton Paar, AMVn 1569).

Fig. 1 shows XRD and cyclic voltammograms of thin oxide films obtained by the sol–gel method. The XRD patterns contained diffraction peaks that were ascribed to spinel-type $LiNi_{0.5}Mn_{1.5}O_4$ (LNMO), Pt substrate and clay. Clay was used to fix the thin-film samples to the sample holder for XRD measurements. Cyclic voltammograms (Fig. 1b) of thin films in an organic electrolyte (1 M $LiClO_4$/PC) show two pairs of redox peaks that correspond to Li^+ insertion/extraction at LNMO thin films.[12,13] These peaks at around 4.75 V (*vs.* Li^+/Li) were observed continuously with the same intensity, which shows that there was no clear degradation of LNMO thin films for 5 cycles. This result confirmed that the sol–gel method gave well-crystallized LNMO thin films.

The electrochemical behaviors of the LNMO thin films in aqueous solutions are shown in Fig. 2. In this study, we used a solution of $LiNO_3$ as a reference since $LiNO_3$ is widely used to make aqueous electrolyte solutions in the literature on ARLBs.[14–16] Wessells *et al.* reported that a solution of $LiNO_3$ showed higher electrochemical stability than those of Li_2SO_4 and LiCl, and an increase in the concentration of $LiNO_3$ (up to 5 M) improved the stability of aqueous electrolytes.[17] In solutions of 0.5 M and saturated $LiNO_3$ (Fig. 2a and b), oxidation currents began to increase at a potential of 1.3 V (*vs.* Ag/AgCl), but there were no clear redox pairs that corresponded to Li^+ insertion/extraction at LNMO thin films. Since the potential of 1.3 V (*vs.* Ag/AgCl), which is equal to 1.91 V (*vs.* reversible hydrogen electrode, RHE) at pH 7, was higher than the upper limit of the window for

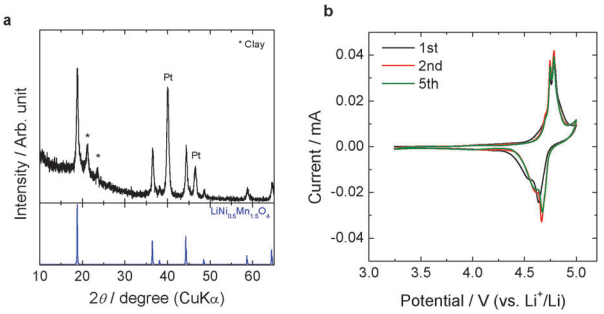

Fig. 1 (a) XRD pattern of LNMO thin film on a Pt substrate and (b) cyclic voltammograms of LNMO in 1 M $LiClO_4$/PC.

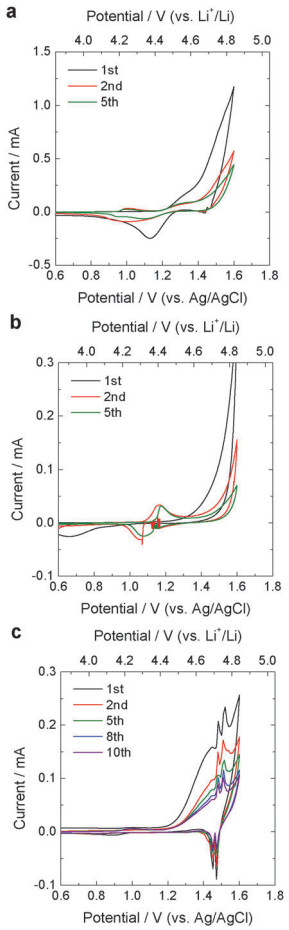

Fig. 2 Cyclic voltammograms of LNMO with aqueous solutions of (a) 0.5 M $LiNO_3$, (b) saturated $LiNO_3$, and (c) 0.25 M Li–PO_4 buffer with saturated PDSS (pH 7).

water (1.23 V *vs.* RHE), the oxidation currents observed on LNMO thin films in $LiNO_3$ solutions were ascribed to the oxygen evolution reaction.

When we added PDSS to a solution of 0.5 M $LiNO_3$, the oxidation current for oxygen evolution was suppressed, and two redox pairs appeared at around 1.5 V (*vs.* Ag/AgCl) (ESI,† Fig. S1). Since this potential is almost the same as that in Fig. 1b, these redox pairs were attributed to Li^+ insertion/extraction of LNMO in the aqueous solution. As we continued potential cycling, however, the redox pairs of Li^+ insertion/extraction were weakened, and they finally disappeared in the 5th cycle. In a neutral aqueous solution, the pH in the vicinity of electrodes should decrease during oxygen evolution, which proceeds as a side reaction:

$$2H_2O \rightarrow O_2 + 4H^+ + 4e^- \quad (1)$$

Therefore, the LNMO thin film gradually dissolved in the low-pH aqueous solution. To obtain stable voltammograms, the protons generated *via* oxygen evolution need to be consumed. In this study, we sought to mitigate the decrease in pH by using a buffer solution. Phosphate buffer stabilizes the proton concentration *via* the following chemical reaction:

$$H_2PO_4^- \leftrightarrows H^+ + HPO_4^{2-} \quad (2)$$

When we used a solution of Li–PO_4 buffer with saturated PDSS, there were clear redox pairs at around 1.5 V (*vs.* Ag/AgCl) (Fig. 2c). The currents of these redox pairs gradually decreased, but were steady in the 10th cycle. This implies that the phosphate buffer effectively reduced the changes in the local pH in the vicinity of the electrodes, and protected the LNMO film from dissolving in the electrolyte.

In the electrolytes with PDSS, we should consider the possibility of Na^+ insertion/extraction at the LNMO electrodes since there are more Na^+ ions than Li^+ ions. Kim and Amatucci investigated Na^+ and Li^+ insertion/extraction on $Ni_{0.5}Mn_{1.5}O_4$, which is a form of fully Li^+-extracted LNMO, and reported that the redox potential of Na^+ insertion was 0.7 V lower than that of Li^+ insertion.[18] Although a redox peak of Na^+ insertion/extraction was expected to appear at 0.8 V (*vs.* Ag/AgCl), there were no clear peaks corresponding to Na^+ insertion/extraction. Two possible hypotheses can be considered to explain the fact that Na^+ insertion/extraction at the LNMO electrodes did not occur in this study. First, the degree of dissociation of PDSS would be small, and elemental sodium would not exist in the form of Na^+ ions. Second, the insertion/extraction rate of Na^+ ions would be slower than that of Li^+ ions. The ionic radius of Na^+ (102 pm) is larger than that of Li^+ (76 pm), and the diffusion coefficient of Na^+ in $Li_4Ti_5O_{12}$, for example, was 110 times lower than that of Li^+.[19] While it is unclear why Na^+ insertion/extraction did not occur on LNMO in PDSS solutions, the presence of PDSS did not interrupt, but rather allowed Li^+ insertion/extraction at the LNMO thin film by suppressing oxygen evolution even in the aqueous solution.

In the electrolyte consisting of phosphate buffer without PDSS, we did not observe Li^+ insertion/extraction, and instead only observed the oxidation current of oxygen evolution (ESI,† Fig. S2). Therefore, PDSS plays an essential role of stabilizing the aqueous electrolyte for high potentials.

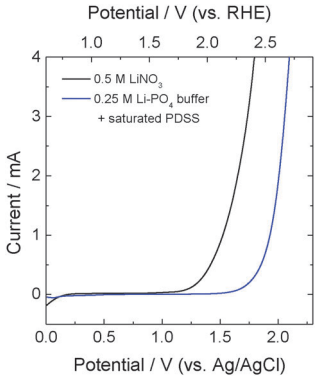

Fig. 3 Linear sweep voltammograms of rotating Pt electrodes in aqueous solutions of 0.5 M $LiNO_3$ and 0.25 M Li–PO_4 buffer with saturated PDSS (pH 7).

The electrochemical stability of aqueous electrolytes was investigated by the RDE method with a Pt disk. We used the RDE method to examine the electrochemical stability of solutions since rotation of the Pt disk allows us to evaluate precisely the onset potential of water oxidation by removing oxygen gas generated from the electrode surface. Fig. 3 shows linear sweep voltammograms of the Pt disk electrode. While the oxidation current began at 1.0 V (*vs.* Ag/AgCl) in the electrolyte of 0.5 M $LiNO_3$, the onset potential of water oxidation shifted positively to 1.6 V (*vs.* Ag/AgCl) in the PDSS buffer solution. This potential corresponds to 2.2 V (*vs.* RHE) and 4.8 V (*vs.* Li^+/Li), implying that PDSS provided a stable aqueous electrolyte, in which LNMO served as a high-voltage positive-electrode material for use in ARLB. In addition, based on the results of impedance spectroscopy, the ionic conductivity of the solution of Li–PO_4 buffer with saturated PDSS was 110 mS cm^{-1} at 25 °C. This value is almost similar to the ionic conductivity of $LiNO_3$ aqueous solutions.[16]

To better understand the mechanism involved in the PDSS effect for improving the stability of aqueous electrolytes, we considered three possible explanations. First, the chemical composition of the LNMO surface was checked with XPS before and after the electrochemical measurements. There was no clear change in the chemical compositions among the three electrodes (ESI,† Table S1 and Fig. S3). All of the electrodes had a large amount of carbon, which was caused by the byproducts (mainly $LiCO_3$) of the sol–gel method. Even after Xe beam etching for 1 min, the chemical composition was unchanged. Therefore, a surface film was not formed in the electrolyte with PDSS.

Second, the physicochemical properties of PDSS solutions were characterized in terms of the ^{1}H-NMR spin–spin relaxation time (T_2). Based on the relaxation curves from the CMPG experiment, the solution of 2.0 M PDSS, which was almost saturated, had a shorter T_2 than the solution of 0.1 mol dm^{-3} PDSS (shown in ESI,† Fig. S4). In the free induction decay (FID) curves, the intensity was increased mainly as a result of water molecules. The relationship between the viscosity (η) and T_2 is summarized in Table S2 (ESI†), and the following dependence was roughly derived:

$$T_2 \propto 1/\sqrt{\eta} \quad (3)$$

A similar correlation was also observed in viscous solutions,[20] and therefore PDSS aqueous solutions did not exhibit any anomalous physicochemical properties. In this study, the bulk properties of PDSS aqueous solutions cannot explain the improvement in the stability of the electrochemical window.

Third, an alternative explanation is based on the enrichment of the electrode surface with anions. Highly concentrated electrolytes containing lithium salts such as LiTFSI and $LiPF_6$ have extraordinary chemical features. McOwen *et al.* reported that anions (*e.g.*, $TFSI^-$ and PF_6^-) accumulated on the surface of positive electrodes with increasing potential and hindered the access of the solvent.[21] The accumulation of anions suppressed the continuous oxidation of solvent molecules.[22] Furthermore, Suo *et al.* also reported that water decomposition was suppressed in a highly concentrated aqueous solution of LiTFSI.[11] Since the PDSS anion was as bulky as the TFSI anion, it is expected that the surface will be effectively covered with PDSS anions. The high concentration of PDSS anions at the electrode–electrolyte interface should serve as a barrier to repel water molecules from the surface of the LNMO electrode. Another advantage of using PDSS as a barrier is that PDSS did not affect the concentration of Li^+ in the electrolytes. While a high concentration of Li salts is useful for improving the electrochemical stability of electrolytes, the use of highly concentrated electrolytes containing Li salts is directly associated with an increase in the redox potential for Li^+ insertion/extraction. According to the Nernst equation shown below (eqn (4)), when the activity of Li^+ cation (a_{Li^+}) increases 10-fold, the redox potential will increase by 59.1 mV (*vs.* standard hydrogen electrode, SHE).

$$E = E^0 + RT/F \ln(a_{Li^+}) \quad (4)$$

where E is the redox potential, E^0 is the formal potential, R is the gas constant, and F is the Faraday constant. A high redox potential is unsuitable for the improved electrochemical window of the electrolyte. Therefore, PDSS is a suitable salt without Li^+ cation since it does not alter the redox potential of Li^+ insertion/extraction on LNMO electrodes.

Since sulfonate ions tend to be strongly adsorbed on a Pt surface, it is possible for adsorbed sulfonate ions to block water molecules from accessing the electrode surface. Fig. S5 (ESI†) shows that the voltammograms for a LNMO thin film grown on an Au substrate are almost the same as those for a LNMO thin film grown on a Pt substrate. The addition of PDSS is applicable not only for a Pt substrate but also for a Au substrate to improve the stability of aqueous electrolytes.

In summary, solutions containing PDSS showed greater stability of the aqueous electrolytes in the presence of high potentials. A wide potential window that extended positively to 1.6 V (*vs.* Ag/AgCl), which offered a stable aqueous electrolyte to enable Li^+ insertion/extraction on LNMO electrodes, was obtained in the solution consisting of PDSS and phosphate buffer. The present work suggests that anions in the electrolyte salts play a pivotal role in stabilizing aqueous electrolytes.

This study was supported by the MEXT program "Elements Strategy Initiative to Form Core Research Center" of the Ministry of Education, Culture, Sports, Science, and Technology (MEXT) of Japan. The authors thank Tosoh Finechem Corporation for supplying PDSS.

Notes and references

1 P. T. Moseley and J. Garche, *Electrochemical Energy Storage for Renewable Sources and Grid Balancing*, Elsevier, 2015.
2 Z. Yang, J. Zhang, M. C. W. Kintner-Meyer, X. Lu, D. Choi, J. P. Lemmon and J. Liu, *Chem. Rev.*, 2011, **111**, 3577–3613.
3 P. G. Balakrishnan, R. Ramesh and T. Prem Kumar, *J. Power Sources*, 2006, **155**, 401–414.
4 H. Kim, J. Hong, K.-Y. Park, H. Kim, S.-W. Kim and K. Kang, *Chem. Rev.*, 2014, **114**, 11788–11827.
5 N. Alias and A. A. Mohamad, *J. Power Sources*, 2015, **274**, 237–251.
6 W. Li, J. R. Dahn and D. S. Wainwright, *Science*, 1994, **264**, 1115–1118.
7 E. Peled, D. Golodnitsky and G. Ardel, *J. Electrochem. Soc.*, 1997, **144**, L208–210.
8 I. B. Stojković, N. D. Cvjetićanin and S. V. Mentus, *Electrochem. Commun.*, 2010, **12**, 371–373.
9 S.-K. Jeong, M. Inaba, Y. Iriyama, T. Abe and Z. Ogumi, *Electrochem. Solid-State Lett.*, 2003, **6**, A13–A15.
10 Y. Yamada, K. Furukawa, K. Sodeyama, K. Kikuchi, M. Yaegashi, Y. Tateyama and A. Yamada, *J. Am. Chem. Soc.*, 2014, **136**, 5039–5046.
11 L. Suo, O. Borodin, T. Gao, M. Olguin, J. Ho, X. Fan, C. Luo, C. Wang and K. Xu, *Science*, 2015, **350**, 938–943.
12 M. Gellert, K. I. Gries, J. Zakel, A. Ott, S. Spannenberger, C. Yada, F. Rosciano, K. Volz and B. Roling, *Electrochim. Acta*, 2014, **133**, 146–152.
13 R. Santhanam and B. Rambabu, *J. Power Sources*, 2010, **195**, 5442–5451.
14 R. Ruffo, C. Wessells, R. A. Huggins and Y. Cui, *Electrochem. Commun.*, 2009, **11**, 247–249.
15 L. Tian and A. Yuan, *J. Power Sources*, 2009, **192**, 693–697.
16 R. Ruffo, F. La Mantia, C. Wessells, R. A. Huggins and Y. Cui, *Solid State Ionics*, 2011, **192**, 289–292.
17 C. Wessells, R. Ruffo, R. A. Huggins and Y. Cui, *Electrochem. Solid-State Lett.*, 2010, **13**, A59–A63.
18 J. R. Kim and G. G. Amatucci, *Chem. Mater.*, 2015, **27**, 2546–2556.
19 M. Kitta, K. Kuratani, M. Tabuchi, R. Kataoka, T. Kiyobayashi and M. Kohyama, *Electrochemistry*, 2015, **83**, 989–992.
20 J.-P. Korb, N. Vorapalawut, B. Nicot and R. G. Bryant, *J. Phys. Chem. C*, 2015, **119**, 24439–24446.
21 D. W. McOwen, D. M. Seo, O. Borodin, J. Vatamanu, P. D. Boyle and W. A. Henderson, *Energy Environ. Sci.*, 2014, **7**, 416–426.
22 J. Vatamanu, O. Borodin and G. D. Smith, *J. Phys. Chem. C*, 2012, **116**, 1114–1121.

